THR-ß agonism improves disease activity and metabolism independent of body weight in a mouse model of non-alcoholic steatohepatitis and fibrosis

Aimo Kannt[1], Paulus Wohlfart[1], Andreas Madsen[2], Sanne Veidal[2], Michael Feigh[2], and Dieter Schmoll[1]

[1]Sanofi-Aventis Deutschland GmbH
[2]Gubra

April 28, 2020

Abstract

Background and Purpose: Activation of hepatic thyroid hormone receptor ß (THR-ß) is associated with systemic lipid lowering, increased bile acid synthesis and fat oxidation. In patients with non-alcoholic steatohepatitis (NASH), treatment with THR-ß agonists led to reduction in hepatic steatosis and circulating lipids, and resolution of NASH. We chose resmetirom (MGL-3196), a liver-directed, selective THR-ß agonist, as a prototype to investigate the effects of THR-ß agonism in mice with diet-induced obesity (DIO) and biopsy-confirmed advanced NASH with fibrosis. Experimental Approach: C57Bl/6J mice were fed a diet high in fat, fructose and cholesterol for 34 weeks, and only biopsy-confirmed DIO-NASH mice with fibrosis were included. Resmetirom was then administered at a daily dose of 3 mg/kg p.o. over a period of eight weeks. Systemic and hepatic metabolic parameters, histological NAFLD activity and fibrosis scores, and liver RNA expression profiles were determined to assess the effect of THR-ß agonism. Key Results: Treatment with resmetirom did not influence body weight but led to significant reduction in liver weight (-43 %, $p<0.001$), hepatic steatosis (-53 %, $p<0.001$), plasma ALT activity (-49 %, $p<0.001$), liver and plasma cholesterol (-27 % and -60 %, respectively, $p<0.001$), and blood glucose (6.3 vs. 7.5 mmol/l, $p<0.001$). These metabolic effects translated into significant improvement in NAFLD activity score. Moreover, lower alpha-smooth muscle actin content and down-regulation of genes involved in fibrogenesis indicated a decrease in hepatic fibrosis. Conclusion and implications: Our model robustly reflected clinical observations of body weight-independent improvements in systemic and hepatic metabolism including anti-steatotic activity.

Bullet Point Summary

What is already known

- Resmetirom reduces hepatic steatosis in patients with non-alcoholic steatohepatitis (NASH)
- Thyroid hormone receptor beta agonists lower circulating and hepatic lipids in models of metabolic disease with fatty liver.

What this study adds

- Resmetirom improves liver health, systemic dyslipidemia and liver histopathology in diet-induced obese mice with biopsy-confirmed NASH and fibrosis without causing weight loss
- Whole genome expression analysis indicates activation of the canonical THR-β signaling pathway and down-regulation of genes involved in fibrogenesis

Clinical Significance

Long-term resmetirom treatment may lead to fibrosis resolution.

Introduction

Non-alcohol fatty liver disease (NAFLD) describes a spectrum of liver abnormalities ranging from fatty liver or simple steatosis to non-alcoholic steatohepatitis (NASH) without or with hepatic fibrosis. NAFLD is a common condition, with a global prevalence of approximately 25 %, strongly linked to obesity, diabetes and systemic dyslipidemia (Younossi, Koenig et al, 2016). NASH is characterized by strong hepatic steatosis, lobular inflammation and hepatocyte ballooning (Diehl and Day, 2017). The prevalence of NASH is increasing (Estes, Razavi et al, 2018; Estes, Anstee et al, 2018), and NASH with advanced fibrosis is associated with a strong increase in liver-related and overall mortality (Ekstedt, Hagström et al, 2015; Dulai, Singh et al, 2017). No pharmacological therapy is approved for the treatment of NASH, though some experimental drugs are currently in later stages of clinical development (Garber, 2019). First-line therapy is lifestyle intervention with a focus on weight loss (Chalasani, Younossi et al, 2018). Thus, new therapies for advanced NASH with fibrosis are urgently needed.

Thyroid hormone receptor ß (THR-ß) is the most abundant thyroid hormone receptor isoform in the liver but also expressed in other tissues. Its expression in the liver is reduced in patients with NASH (Krause, Grohs et al, 2018). Activation of hepatic THR-ß is associated with systemic lipid lowering, increased bile acid synthesis and fat oxidation (Sinha, Bruinstroop et al, 2019). Liver-directed agonists with high selectivity for THR-ß over THR-α have been generated (Kelly, Pietranico-Cole et al, 2014; Erion, Cable et al, 2007) and showed metabolic benefits in preclinical models of diabetes and obesity including reduced hepatic steatosis and inflammation (Sinha, Bruinstroop, et al, 2019). However, there is little information on their activity in obese animals with manifest NASH and fibrosis. Recently, resmetirom (MGL-3196) was evaluated in a 36-week clinical phase-2 study in patients with biopsy-confirmed NASH, was well tolerated and led to a significant reduction in hepatic fat fraction, circulating LDL cholesterol and triglycerides, and a higher rate of NASH resolution compared to placebo (Harrison, Bashir et al, Lancet 2019).

Here we report the evaluation of resmetirom as a prototype of a liver-directed, selective THR-ß agonist in a diet-induced obese (DIO) and biopsy-confirmed mouse model of advanced NASH with fibrosis. Our results reflect clinical findings of reduced hepatic steatosis, liver injury, circulating cholesterol and histological NAFLD activity score (NAS). In addition, we demonstrate changes in expression of THR-ß regulated genes. Of note, these effects were observed at a low dose of 3 mg/kg that was not associated with body weight loss. This is, to our knowledge, the first study describing the effects of resmetirom in a pre-clinical model of NASH, fully replicating recent clinical observations.

Methods

The effect of THR-ß agonism was investigated in mice with diet-induced obesity and biopsy-confirmed NASH and fibrosis (DIO-NASH model) as described by Kristiansen et al. (2016). All animal experiments were conducted according to the international principles for care and use of laboratory animals and were covered by personal licenses for Jacob Jelsing (2013-15-2934-00784 and 2015-15-0201-00518) issued by the Danish committee for animal research.

Thirty-six male C57BL/6J mice (5 weeks old), obtained from JanVier (JanVier Labs, France), were included in the study. Before treatment with resmetirom, animals had *ad libitum* access for 34 weeks to a regular rodent diet (Altromin 1324, Brogaarden, Denmark) or a diet high in fat (40%), of these 18% trans-fat, 40% carbohydrates (20% fructose) and 2% cholesterol (D09100301, Research Diet, United States) previously described as the AMLN diet (Clapper, Hendricks, et al, 2013) and tap water.

The study design is illustrated in figure 1a. A baseline liver biopsy was conducted 3 weeks before the intervention for histological assessment of individual fibrosis (stage [?]1) and steatosis (score [?]2), as described (Kristiansen et al., 2016). A week before the intervention the animals were randomized and stratified according to liver Col1a1 quantification into three groups: Group 1, Lean-chow control (n=12); Group 2, DIO-NASH vehicle (n=12); Group 3, DIO-NASH + resmetirom (n=12). Resmetirom (MGL-3196) was purchased from MedChemExpress (catalog no. HY-12216) and administered once daily, in the morning, by oral gavage at a dose of 3 mg/kg. The vehicle used for compound formulation and control injections was

0.6% methyl cellulose with 0.5% Tween 80. The resmetirom concentration in the dosing solution was 0.6 mg/ml, injection volume was 5 ml per kg body weight. The intervention lasted for a period of 8 weeks. At the end of the intervention animals were euthanized and liver tissue and plasma were collected.

Body weight determination, body composition analysis, blood sampling, plasma biochemistry, endotoxin determination and liver tissue biochemistry were performed as previously described (Kristiansen, Veidal, et al, 2016). Statistical significance for the difference to the vehicle control group was assessed using a one-sided ANOVA with Dunnett's test.

For histology, baseline liver biopsy and terminal samples were collected from the left lateral lobe (about 50-100 mg at baseline and 200 mg at the end) and fixed overnight in 4% paraformaldehyde. Liver tissue was paraffin embedded and sectioned (3µm thickness). Sections were stained with Hematoxylin and Eosin and Sirius Red to assess hepatic steatosis and fibrosis respectively, followed by analysis with Visiomorph software (Visiopharm, Denmark). Collagen 1 alpha 1 (col1a1), α-smooth muscle actin (α-SMA) and galectin-3 were assessed by quantitative immunohistochemistry staining using anti-col1a1 (1:300; Southern Biotech, Birmingham; secondary antibody Bright Vision anti-goat, ImmunoLogic, Netherlands), anti-α-SMA (1:800; Abcam, Cambridge, UK; secondary antibody Envision rabbit, Agilent Technologies, Glostrup, Denmark) or anti-galectin-3 (gal-3; 1:50000; Biolegend, San Diego, United States; secondary antibody anti-rat IgG 1:800, VWR, Soeborg, Denmark; Envision rabbit, Agilent Technologies, Glostrup, Denmark) as described (Kristiansen, Veidal, et al, 2016). A pathologist blinded to the study performed the histological assessment and scoring. NAFLD activity score (NAS) combining steatosis, lobular inflammation and hepatocyte ballooning scores, and fibrosis stage were quantified applying the criteria proposed by Kleiner, Brunt, et al. (2005). Statistical significance for a difference in the number of animals showing improvement or worsening was evaluated using a one-sided Fisher's exact test with Bonferroni correction with the DIO-NASH vehicle group as comparator.

Liver tissue was harvested from the left lateral lobe, stabilized overnight in RNAlater® solution (Merck KGaA, Darmstadt, Germany) and stored at -80 °C. Total RNA isolation was performed with the RNeasy kit following the instructions of the manufacturer (QIAGEN GmbH, Hilden, Germany). Quantity and integrity of purified RNA was measured with an Agilent RNA 6000 Nano kit using an Agilent 2100 Bioanalyzer (Agilent Technologies Inc, Waldbronn, Germany). Paired-end sequencing was performed using a TruSeq mRNA Library-Kit (Illumina, San Diego, CA, USA) at Atlas Biolabs, Berlin, Germany, with a sequencing depth of 80 to 100 million reads per sample. RNA sequencing raw data were analyzed using a software package and standardized RNA Seq analysis workflow (Array Studio Version 10.1.3.3, Omicsoft Qiagen). This workflow included alignment to a reference mouse gene model, quantification, normalization, and finally detection of differentially expressed genes using the DESeq2 module (Costa-Silva, Domingues & Lopez, 2017). Results were corrected for variable multiplicity and false-discovery rate (FDR) adjusted p-values calculated using the Benjamini-Hochberg correction (Benjamini & Hochberg, 1995). Differentially expressed gene data were further interrogated on pathways and further causal relationship through the use of Ingenuity Pathway Analysis (Ingenuity Qiagen) as described in Krämer, Green, et al. (2014).

Results

Figure 1b shows the change in body weight over the treatment period of eight weeks. Resmetirom had no effect on weight or food intake (figure 1c). Body weight remained stable throughout the treatment period; transient weight loss observed at day 39 in all three groups resulted from the four-hour fasting period before taking blood for glucose determination.

THR-ß agonism had a profound effect on plasma transaminase activities, leading to a reduction by about 50 % for ALT and 26 % for AST compared to DIO-NASH vehicle controls (figures 2a and 2b). Plasma total cholesterol levels that were strongly elevated in DIO-NASH mice compared to lean controls nearly normalized upon treatment with resmetirom (figure 2c). There was a trend towards lower plasma triglycerides that was, however, not statistically significant (p=0.052, figure 2d). Four-hour fasting blood glucose levels determined on treatment day 39 were significantly lower in resmetirom-treated animals (figure 2e) whereas resmetirom

had no influence on plasma insulin concentration (figure 2f).

Liver hypertrophy observed in DIO-NASH mice was markedly reduced upon treatment with the THR-ß agonist (figure 3a), accompanied by a strong reduction in liver triglycerides, total cholesterol and hepatic total lipid content (figures 3b-d). Liver col1a1 and α-SMA contents were lower after resmetirom treatment (figures 3e and f). The difference to vehicle-treated DIO-NASH mice remained statistically significant upon normalization to liver weight for α-SMA but not for col1a1 (not shown).

Resmetirom treatment was associated with changes in liver morphology (figure 4a, b) and a significant improvement (post-treatment vs. pre-treatment biopsy) in the histological NAFLD activity score (NAS) relative to DIO-NASH mice not exposed to the drug (figure 4c). Whereas in DIO-NASH controls, two out of eleven mice had a lower NAS after the intervention period, ten out of twelve resmetirom-treated mice showed an improved NAS (figure 4c), in seven cases by more than one point. Fibrosis staging (pre-post) was lower in two out of twelve mice on resmetirom whereas no change was observed in vehicle-treated DIO-NASH control mice (difference not statistically significant, figure 4d).

Results of hepatic gene expression analysis by RNASeq are summarized in figure 5. In a principal component analysis (PCA) of global gene expression, DIO-NASH vehicle-treated animals separated from lean control animals along the first two principal components (PC1) and (PC2),with resmetirom treatment leading to a separation along PC2 towards values observed in lean control mice (figure 5a). Among 53431 transcripts assessed by RNA Sequencing, DIO-NASH vehicle-treated mice demonstrated a >1.5-fold upregulation of 4614 genes (supporting information, figure S1a) in comparison to lean control animals. Only a fraction of these up-regulated genes (112 of 4614) was significantly reversed by treatment with resmetirom (supporting information, figure S1b and table S1). Furthermore, DIO-NASH vehicle-treated mice demonstrated a differential downregulation (>1.5-fold) of 1750 genes in comparison with lean control mice, with 79 of these transcripts being significantly reversed by resmetirom treatment. Notably, pathway analysis confirmed that changes in gene expression upon resmetirom treatment are consistent with THR-β activation (figure 5b). Compared to DIO-NASH vehicle control animals, THR-β target genes such as deiodinase 1 (Dio1), malic enzyme 1 (Me1), cytochrome P450 7A1 (Cyp7a1) and glycerolphosphate dehydrogenase 2 (Gpd2) were found to be strongly upregulated (figure 5c). Lower expression of fibrosis marker genes collagen 1a1 (Col1a1), α-SMA (Acta2), lysyl oxidase-like 2 (Loxl2) and hydroxysteroid 17-beta dehydrogenase 13 (Hsd17b13, figure 5d) indicates a decrease in incident fibrogenesis which is also reflected in lower col1a1 and α-SMA protein levels (figures 3e, f), although not enough to significantly improve the histological fibrosis staging (figure 4d) within the observed treatment period. Other genes that were recently identified as markers of hepatic fibrosis or hepatocellular carcinoma such as Lipopolysaccharide-binding protein (Lbp; Nien, Sheu, et al, 2019), ATP-binding cassette C3 (Abcc3; Carrasco-Torres, Fattel-Fazenda, et al, 2016) and fatty-acid binding protein 4 (Fabp4; Thompson, Austin, et al, 2018) were markedly downregulated upon treatment with resmetirom (figure 4e). Of note, genes related to fatty acid synthesis (Acaca, Acacb, Fasn), lipolysis (Pnpla2, Lipe, Mgll) and fatty acid oxidation (Cpt1a, Pgc1a, Hadhb) were not found to be regulated upon resmetirom treatment compared to vehicle-treated DIO-NASH mice (supporting information, figure S2).

Discussion

Here we report that the liver-selective THR-ß agonist resmetirom, administered at a dose that does not influence body weight or food intake, has a profound effect on hepatomegaly, hepatic steatosis, liver injury, circulating cholesterol and the histological NAFLD activity score in a diet-induced obese and biopsy-confirmed mouse model of advanced NASH with fibrosis. Our study was performed as an intervention (therapeutic) study in DIO-NASH mice with established metabolic disease also comprising obesity, hypercholesterolemia and insulin resistance, reflecting clinical characteristics of patients with NASH.

Our results are in remarkable agreement with a recently reported phase 2 trial of resmetirom in patients with NASH in which, after 36 weeks of treatment, a forty percent reduction in hepatic fat content measured by magnetic resonance imaging was observed that was accompanied by a significant improvement in circulating

liver transaminases, total and LDL cholesterol. Furthermore, resmetirom responders that had lower hepatic fat fractions at 36 weeks also exhibited significantly reduced NAFLD activity scores (Harrison, Bashir, et al, 2019).

Several THR-ß agonists have been investigated in animal models of metabolic disease with fatty liver (reviewed in Sinha, Bruinstroop, et al, 2019). Sobetirome (GC-1) and eprotirome (KB2115), for example, reduced hepatic steatosis and liver triglycerides in ob/ob mice (Martagon, Lin, et al, 2015). Notably, at the selected doses, treatment also resulted in significant body weight loss, and ob/ob mice do not develop manifest NASH or hepatic fibrosis under the investigated conditions. Similarly, both compounds, administered over a period of ten days, led to strong reductions in liver triglyceride content in Sprague-Dawley rats on a high-fat diet (Vatner, Weismann, et al, 2013) that, however, did not develop NASH. Sobetirome also caused a marked decrease in hepatic and circulating triglycerides and serum ALT in rats fed a high-fat, methionine- and choline-deficient diet (Perra, Simbula, et al, 2008). However, treatment was accompanied by weight loss, and the presence of NASH was not investigated. MB07344/VK2809, a THR-β agonist prodrug selectively taken up by the liver and converted into the active principle, reduced hepatic triglycerides and serum lipids in C57BL/6 mice on a high-fat diet and in Zucker diabetic fatty rats (Erion, Cable, et al, 2007; Cable, Finn, et al, 2009), in the absence of NASH and fibrosis. Thus, there is evidence from several models of metabolic disease for an improvement in liver fat and circulating lipids. Our results add to his body of evidence by showing that THR-β agonism can reduce hepatic steatosis and liver injury in a diet-induced obese model combining metabolic syndrome with advanced NASH and fibrosis.

Multiple preclinical models of NAFLD have been described that vary in their translatability to the human situation (Hansen, Feigh, et al, 2017). Our data indicate that with respect to THR-β agonism, data obtained in biopsy-confirmed DIO-NASH mice have a good human translatability. So far, it is not established to which extent resmetirom is able to also hold or to reverse fibrosis in late-stage NAFLD. In the recent phase 2 trial of resmetirom in patients with NASH and predominantly mild fibrosis, no significant improvement was observed (Harrison, Bashir, et al, 2019). It is unclear whether this results from lack of efficacy or whether the treatment duration of 36 weeks was too short to elicit an observable improvement in hepatic fibrosis. Similar to the population investigated in this trial, our model shows mild fibrosis (approximately 60% F2, 40% F3, see fig. 4d) and no significant improvement in fibrosis score was seen with resmetirom. However, reduced expression of markers of fibrogenesis in resmetirom vs. vehicle-treated DIO-NASH animals indicates an antifibrotic effect of THR-β agonism that may translate into a more robust reduction in fibrosis upon longer duration of treatment. We also speculate that longer pre-feeding with the AMLN diet might further aggravate advanced fibrosis in DIO-NASH mice and could be a useful model for preclinical evaluation of the compound with respect to anti-fibrotic efficacy.

Of note, although our whole genome expression analysis indicated activation of the canonical THR-β pathway, the data did not explain the strong reduction of hepatic lipids by resmetirom as there was no clear down-regulation of fatty acid synthesis genes or stimulation of genes associated with fat oxidation. Thus, the anti-steatotic effect of the compound in this model is not due to transcriptional effects. We speculate that THR-β agonism redirects metabolic fluxes by post-transcriptional and allosteric mechanisms.

An important limitation of our study is the restriction to a single dose level. The dose of 3 mg/kg was selected based on a previous study in DIO mice over 23 days where this dose led to ˜60% reduction in circulating cholesterol levels (Kelly, Pietranico-Cole, et al, 2014). Whereas at the chosen dose of resmetirom showed a marked improvement in hepatic and systemic metabolic health in the absence of obvious adverse effects, additional studies investigating multiple doses will be required to, e.g., establish the maximal tolerated or minimally or maximally effective doses of resmetirom for the treatment of NASH.

Acknowledgements

Claire Kammermeier is gratefully acknowledged for excellent technical assistance.

Conflict of Interest

A.K., P. W. and D.S. are employees of Sanofi. A.N.M., S.S.V. and M.F. are employees of Gubra.

References

Benjamini, Y. & Hochberg, Y. (1995) Controlling the false discovery rate: A practical and powerful approach to multiple testing.*Journal of the Royal Statistical Society B,* **57** , 289-300

Baandrup Kristiansen, M. N. , Veidal, S. S., Christoffersen, C., Feigh, M., Vrang, N., Roth, J. D., . . . , Jelsing, J. (2019) Validity of biopsy-based drug effects in a diet-induced obese mouse model of biopsy-confirmed NASH. *BMC Gastroenterology,* **19** , 228

Chalasani, N., Younossi, Z., Lavine, J. E., Charlton, M., Cusi, K., Rinella, M., . . . , Sanyal, A.J. (2018) The diagnosis and management of nonalcoholic fatty liver disease: Practice guidance from the American Association for the Study of Liver Diseases. *Hepatology,**67,*** 328-357

Clapper, J. R., Hendricks, M. D., Gu, G., Wittmer, C., Dolman, C. S., Herich, J., . . . , Roth, J. D. (2013) Diet-induced mouse model of fatty liver disease and nonalcoholic steatohepatitis reflecting clinical disease progression and methods of assessment. *American Journal of Physiology - Gastrointestinal and Liver Physiology* , **305** , G483-95

Costa-Silva, J., Domingues, D., & Lopes, F.M. (2017) RNA-Seq differential expression analysis: An extended review and a software tool. *PLoS One* , **12** , e0190152.

Diehl, A.M., & Day, C. (2017) Cause, Pathogenesis, and treatment of nonalcoholic steatohepatitis. *New England Journal of Medicine,**377*** , 2063-2072

Dulai, P.S., Singh, S., Patel, J., Soni, M., Prokop, L. J., Younossi, Z., . . . , Loomba, R. (2017) Increased risk of mortality by fibrosis stage in nonalcoholic fatty liver disease: Systematic review and meta-analysis. *Hepatology,* **65** , 1557-1565

Ekstedt, M., Hagström, H., Nasr, P., Fredrikson, M., Stal, P., Kechagias, S., & Hultcrantz, R. (2015) Fibrosis stage is the strongest predictor for disease-specific mortality in NAFLD after up to 33 years of follow-up. *Hepatology,* **61** , 1547–1554

Erion, M. D., Cable, E. E., Ito, B. R., Jiang, H., Fujitaki, J. M., Finn, P. D., . . . , Linemeyer, D. L. (2007) Targeting thyroid hormone receptor-beta agonists to the liver reduces cholesterol and triglycerides and improves the therapeutic index. *Proceedings of the National Academy of Sciences of the United States of America,***104** :15490-15495

Estes, C., Anstee, Q. M., Arias-Loste, M. T., Bantel, H., Bellentani, S., Caballeria, J.,. . . ,Razavi, H. (2018) Modeling NAFLD disease burden in China, France, Germany, Italy, Japan, Spain, United Kingdom, and United States for the period 2016-2030. *Journal of Hepatology,* **69** *,* 896-904

Estes, C., Razavi, H., Loomba, R., Younossi, Z., & Sanyal, A.J. (2018) Modeling the epidemic of nonalcoholic fatty liver disease demonstrates an exponential increase in burden of disease. *Hepatology,***67** , 123-133

Garber, K. (2019) The new liver epidemic. *Nature Biotechnology,***37** , 209-214

Carrasco-Torres, G., Fattel-Fazenda, S., Lopez-Alvarez, G. S., Garcia-Roman, R., Villa-Trevino, S., Vasquez-Garzon, V. R. (2016) The transmembrane transporter ABCC3 participates in liver cancer progression and is a potential biomarker. *Tumour Biology,* **37** , 2007-2014

Hansen, H. H., Feigh, M., Veidal S. S., Rigbolt, K. T., Vrang, N., & Fosgerau, K. Mouse models of nonalcoholic steatohepatitis in preclinical drug development. *Drug Discovery Today* , **22** , 1707-1718

Harrison, S.A., Bashir, M.R., Guy, C.D., Zhou, R., Moylan, C.A., Frias, J.P., . . . , Moussa, S. E. (2019) Resmetirom (MGL-3196) for the treatment of non-alcoholic steatohepatitis: a multicentre, randomised, double-blind, placebo-controlled, phase 2 trial. *The Lancet,***394** , 2012-2024.

Kelly, M. J., Pietranico-Cole, S., Larigan, J. D., Haynes, N. E., Reynolds, C. H., Scott, N., ..., Tilley J. (2014) Discovery of 2-[3,5-dichloro-4-(5- isopropyl-6-oxo-1,6-dihydropyridazin-3-yloxy)phenyl]-3,5-dio xo-2,3,4,5- tetrahydro[1,2,4]triazine-6-carbonitrile (MGL-3196), a Highly Selective Thyroid Hormone Receptor beta agonist in clinical trials for the treatment of dyslipidemia. *Journal of Medicinal Chemistry* **57** , 3912-3923.

Kleiner, D.E., Brunt, E.M., Van Natta, M., Behling, C., Contos, M.J., Cummings, O.W., ..., Sanyal, A. J. (2005) Design and validation of a histological scoring system for nonalcoholic fatty liver disease.*Hepatology,* **41** , 1313-1321

Kramer, A., Green, J., Pollard, J. Jr, & Tugendreich, S. (2014) Causal analysis approaches in Ingenuity Pathway Analysis.*Bioinformatics,* **30** , 523-530.

Krause, C., Grohs, M., El Gammal, A. T., Wolter, S., Lehnert, H., Mann, O., Mittag, J., & Kirchner, H. (2018) Reduced expression of thyroid hormone receptor β in human nonalcoholic steatohepatitis.*Endocrine Connections* **7** , 1448-1456

Kristiansen, M. N., Veidal, S. S., Rigbolt, K. T., Tølbøl, K. S., Roth, J. D., Jelsing, J., Vrang, N., & Feigh, M. (2016) Obese diet-induced mouse models of nonalcoholic steatohepatitis-tracking disease by liver biopsy. *World Journal of Hepatology* , **8** , 673-84

Martagon, A. J., Lin, J. Z., Cimini, S. L., Webb, P., & Phillips, K. J. (2015) The amelioration of hepatic steatosis by thyroid hormone receptor agonists is insufficient to restore insulin sensitivity in ob/ob mice.*PLoS One* **10** , e0122987

Nien, H. C., Sheu, J. C., Chi, Y. C., Chen, C. L., Kao, J. H., & Yang, W. S. (2018) One-year weight management lowers lipopolysaccharide-binding protein and its implication in metainflammation and liver fibrosis. *PLoS One* **13** , e0207882

Perra, A., Simbula, G., Simbula, M., Pibiri, M., Kowalik, M. A., Sulas, P., ..., Columbano, A. (2008) Thyroid hormone (T3) and TRβ agonist GC-1 inhibit/reverse nonalcoholic fatty liver in rats. *The FASEB Journal* **22** , 2981-2989

Sinha, R. A., Bruistroop, E., Singh, B. K., & Yen, P. M. (2019) Nonalcoholic Fatty Liver Disease and Hypercholesterolemia: Roles of Thyroid Hormones, Metabolites, and Agonists. *Thyroid,**29*** , 1173-1191

Thompson, K. J., Austin, R. G., Nazari, S. S., Gersin, K. S., Iannitti, D. A., McKillop, I. H. (2018) Altered fatty acid-binding protein 4 (FABP4) expression and function in human and animal models of hepatocellular carcinoma. *Liver International* **38** , 1074-1083

Vatner, D. F., Weismann, D., Beddow, S. A., Kumashiro, N., Erion, D. M., Liao, X. H., ..., Samuel, V. T. (2013) Thyroid hormone receptor-β agonists prevent hepatic steatosis in fat-fed rats but impair insulin sensitivity via discrete pathways. *American Journal of Physiology - Endocrinology and Metabolism* **305** , E89-100

Younossi, Z. M., Koenig, A. B., Abdelatif, D., Fazel, Y., Henry, L., & Wymer, M. (2016) Global epidemiology of nonalcoholic fatty liver disease-Meta-analytic assessment of prevalence, incidence, and outcomes.*Hepatology,* **64** , 73–84

Figure legends

Figure 1. ***(a)*** Study design. (b) Body weight development over the intervention period. (c) Food intake over the course of the study. ***p<0.001 vs DIO-NASH vehicle control.

Figure 2. Systemic safety and metabolic parameters. (a) Plasma ALT, (b) plasma AST activities. (c) Plasma total cholesterol, (d) plasma triglycerides, (e) 4-hour fasting blood glucose and (f) plasma insulin levels. (a) -(d) were measured at study termination, (e) and (f) on study day 39. *p<0.05, **p<0.01, ***p<0.001 vs DIO-NASH vehicle control.

Figure 3. Liver weight, hepatic lipid, collagen and α-smooth muscle actin (α-SMA) content at study termination. (a) Wet liver weight, (b) hepatic triglycerides, (c) hepatic total cholesterol. (d) Total liver lipid content, (e) hepatic collagen 1a1 and (f) liver α-SMA determined by histology and quantitative image analysis. **p<0.01, ***p<0.001 vs. DIO-NASH vehicle control.

Figure 4. (a) Representative images of liver morphology at termination of the study. H&E staining (20x, scale bar = 100 μm), (b) Picrosirius Red staining (20x, scale bar = 100 μm). (c) Change in NAFLD activity score (pre- vs. post-treatment) for individual animals in the different treatment groups: Lean control mice (grey), DIO-NASH vehicle controls (black) and DIO-NASH mice treated with resmetirom (orange), (d) Change in fibrosis stage as above. N=10-11 per group, **p<0.01 vs DIO-NASH vehicle group (One-sided Fisher's exact test with Bonferroni correction).

Figure 5. Hepatic gene expression assessed by RNA sequencing with subsequent Ingenuity pathway analysis: (a) principal component analysis over all 53431 measured transcripts displaying the first two main components, PC1 and PC2. (b) Visualization of upstream factor analysis performed with Ingenuity, which predicts THR-ß as one important factor activated in the resmetirom treated group. (c-e) Expression of selected genes in normalized counts (FKPM) and shown as box-whisker blots with median (line) and mean (+) and confidence intervals of 5% to 95%. *p<0.05, **p<0.01, *p<0.001 vs DIO-NASH vehicle group (false-discovery rate adjusted for multiplicity by Benjamini-Hochberg correction).

(a)

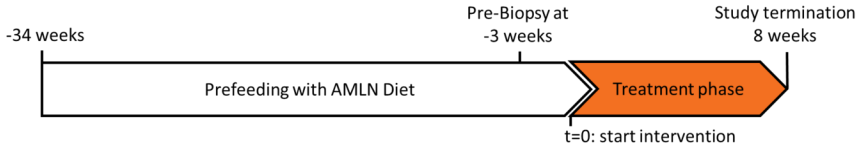

(b)

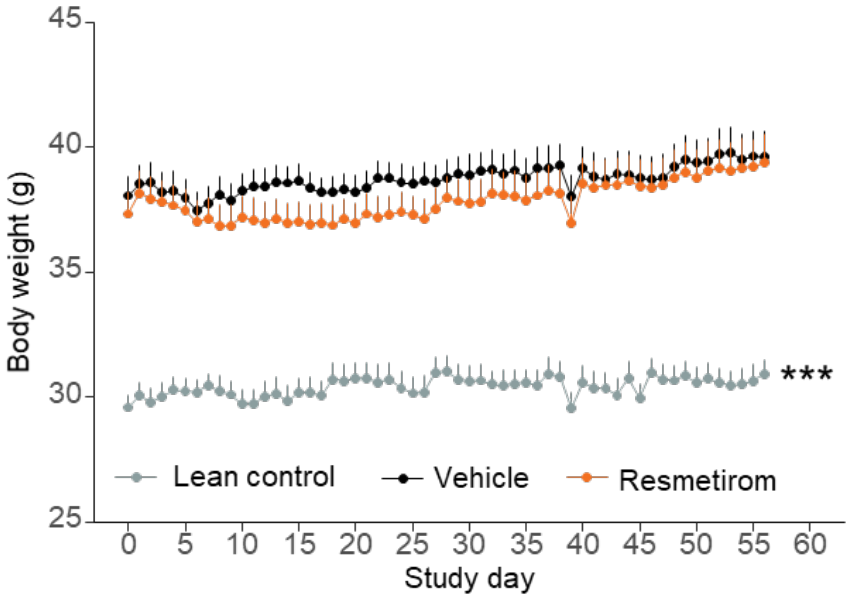

(c)

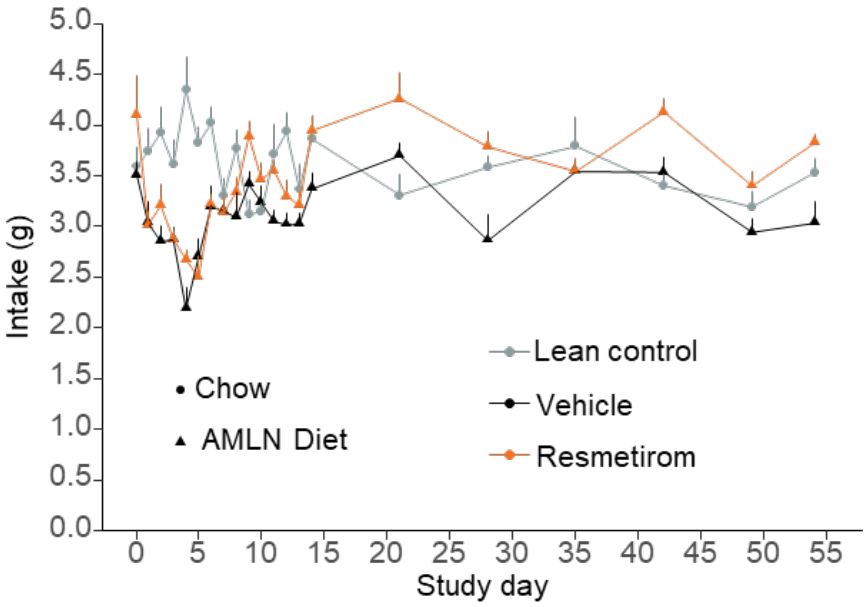

Figure 1

(a) (b)

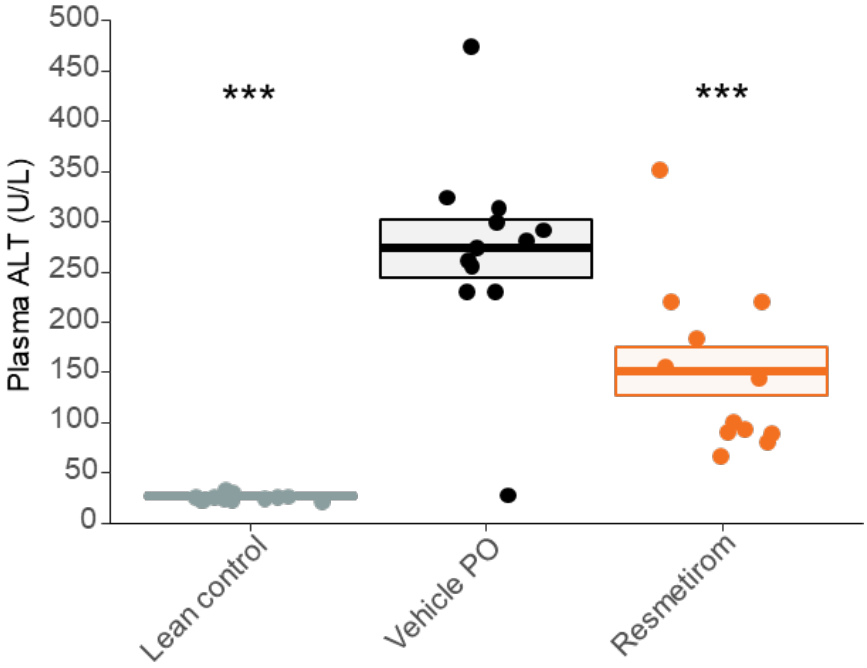

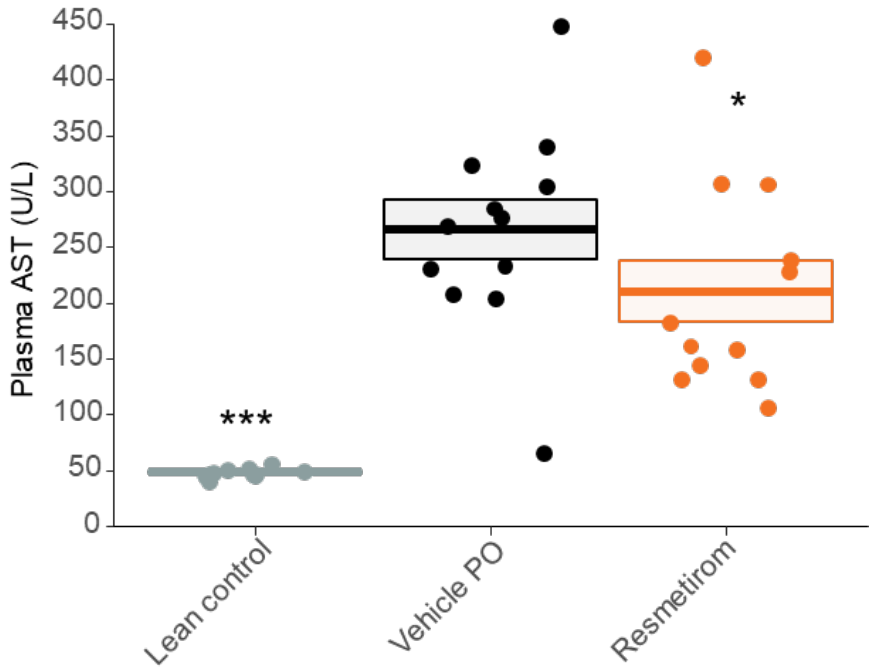

(c) (d)

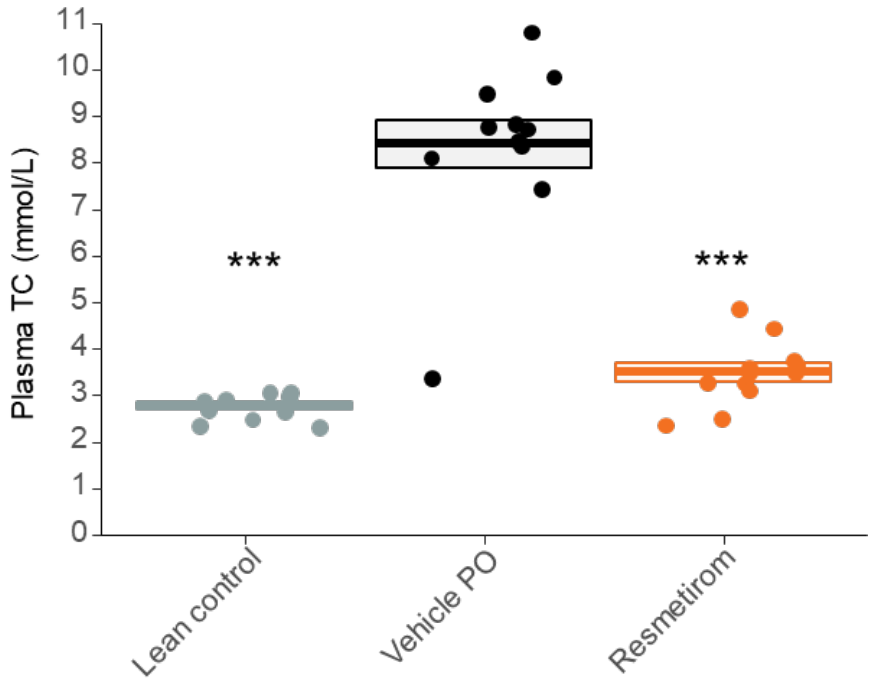

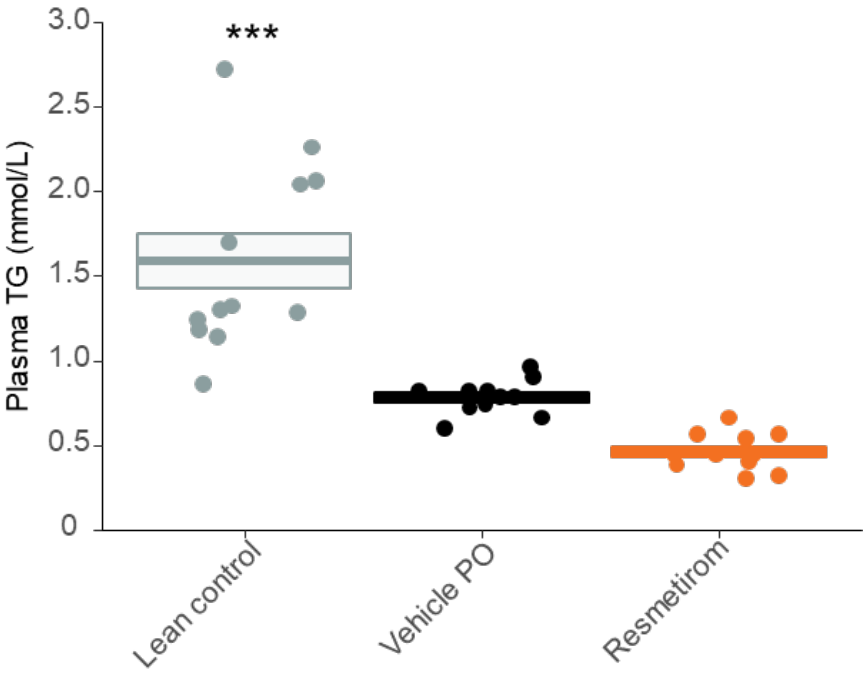

(e) (f)

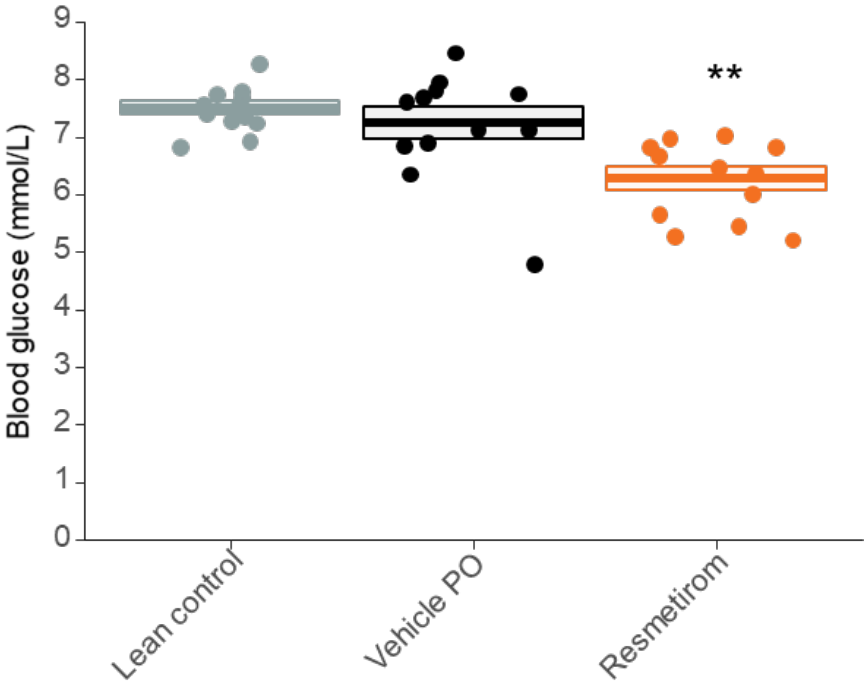

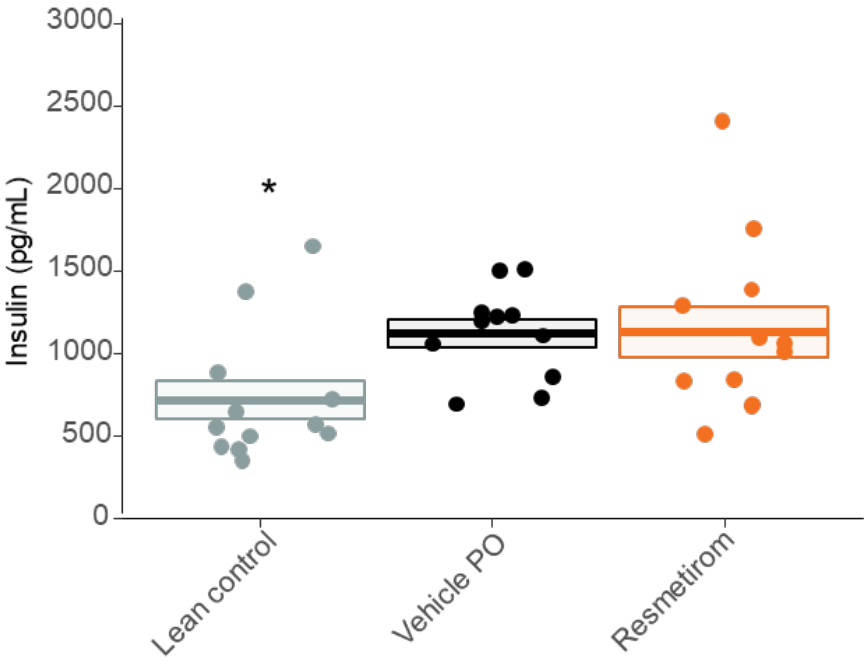

Figure 2

(a) (b)

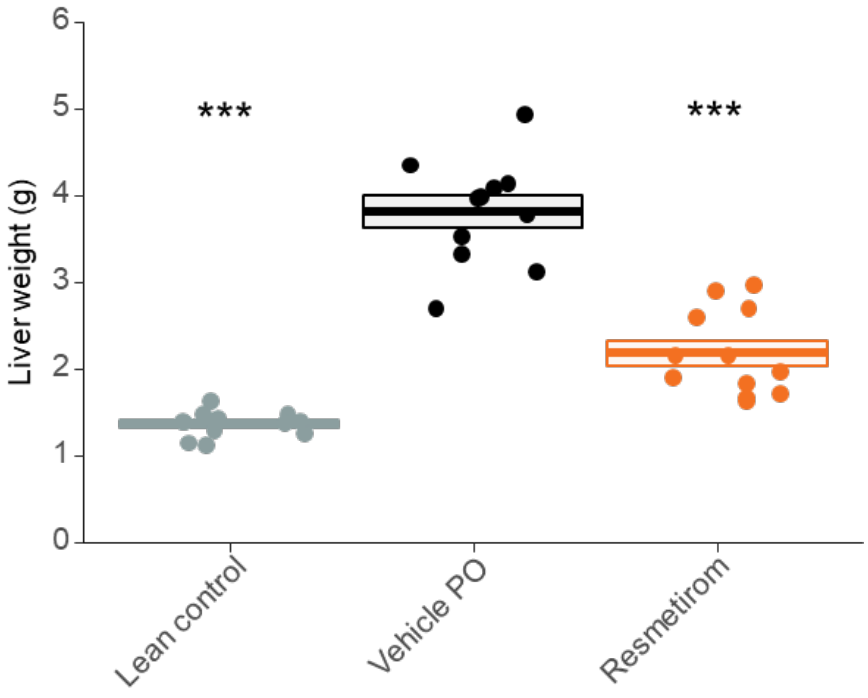

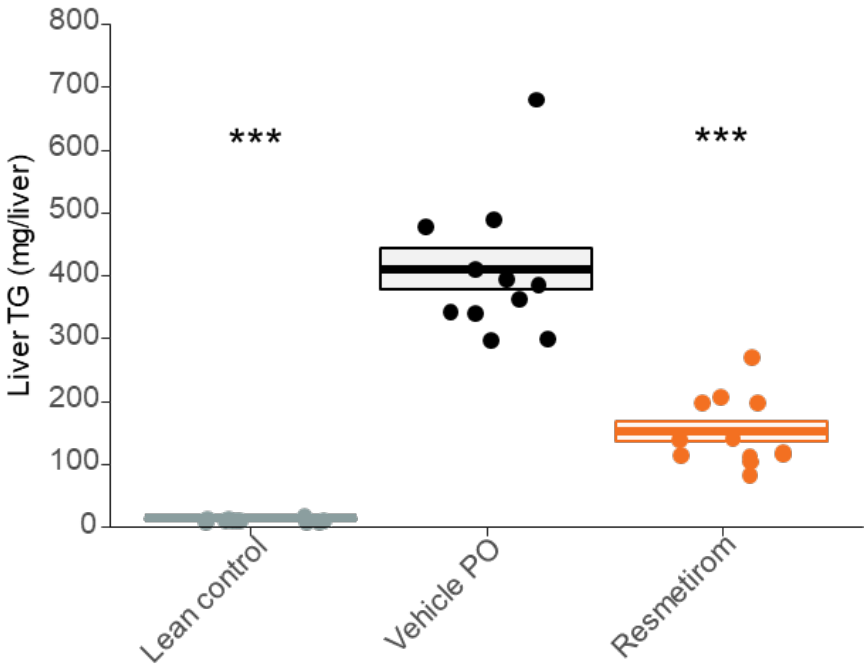

(c) (d)

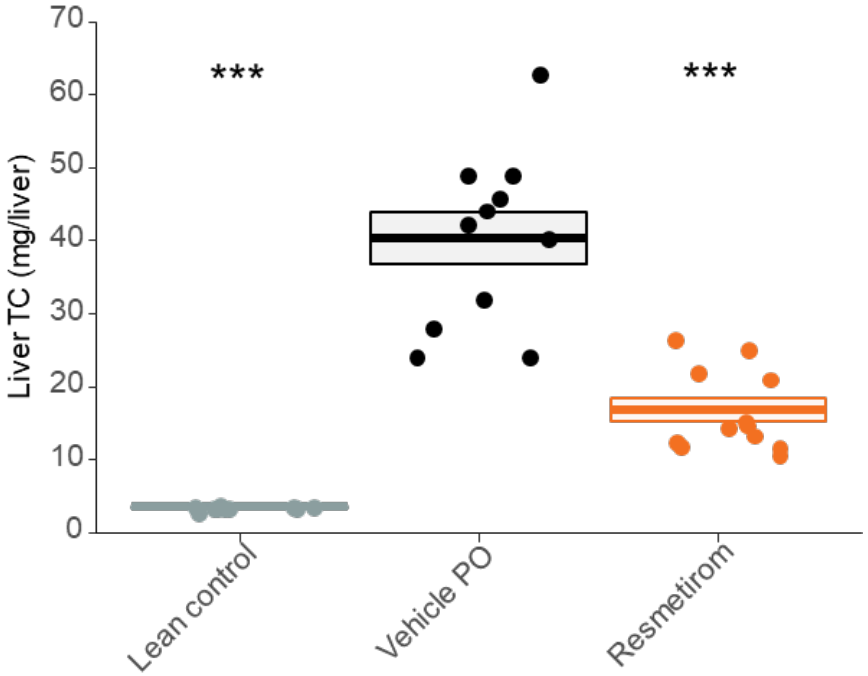

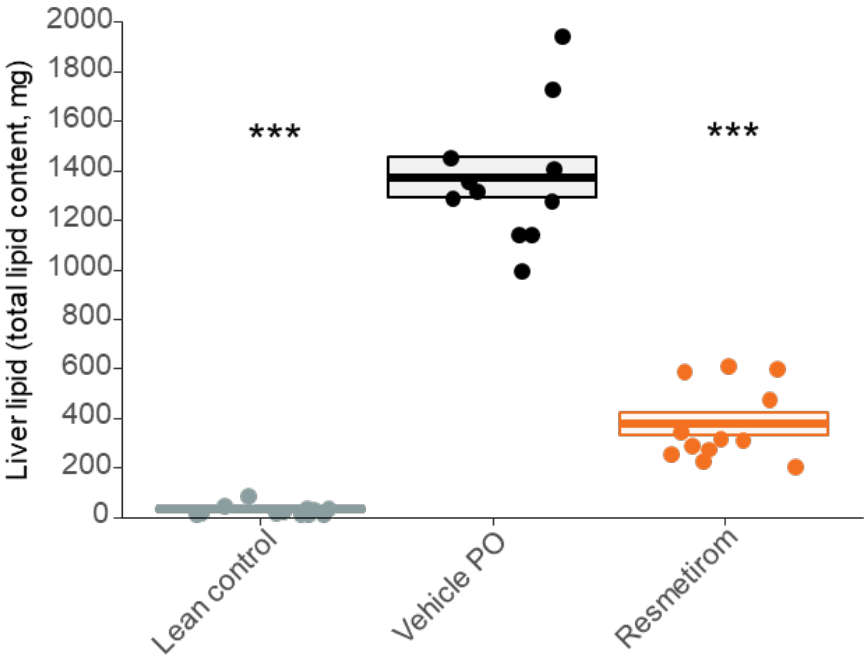

(e) (f)

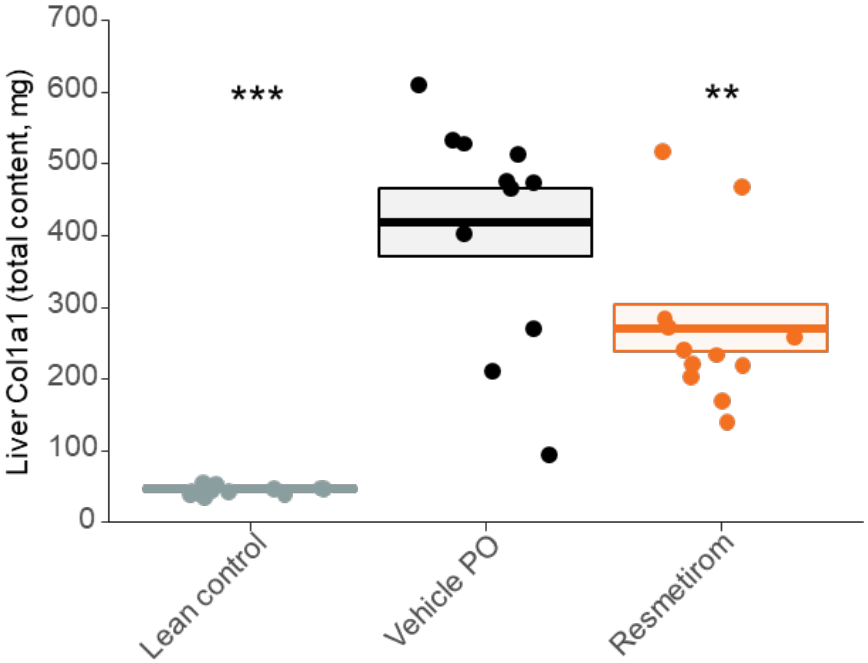

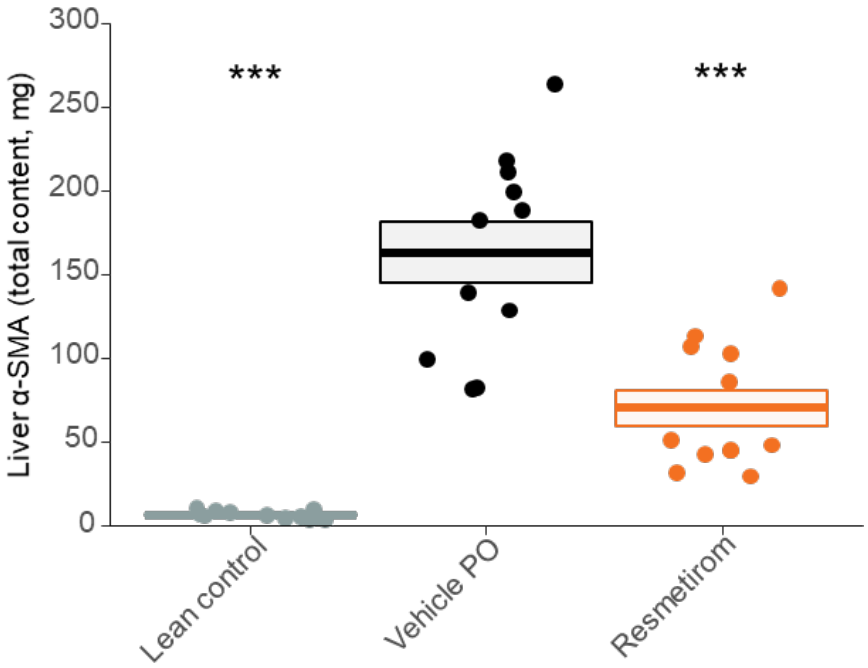

Figure 3

(a)

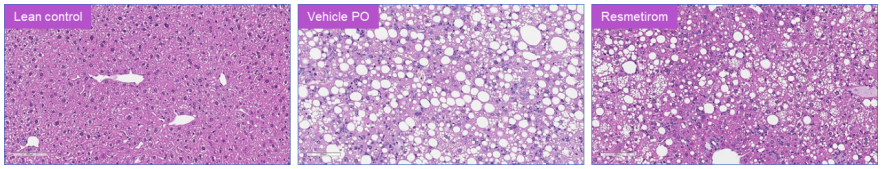

(b)

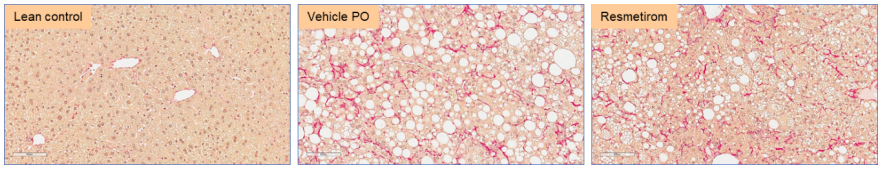

(c) (d)

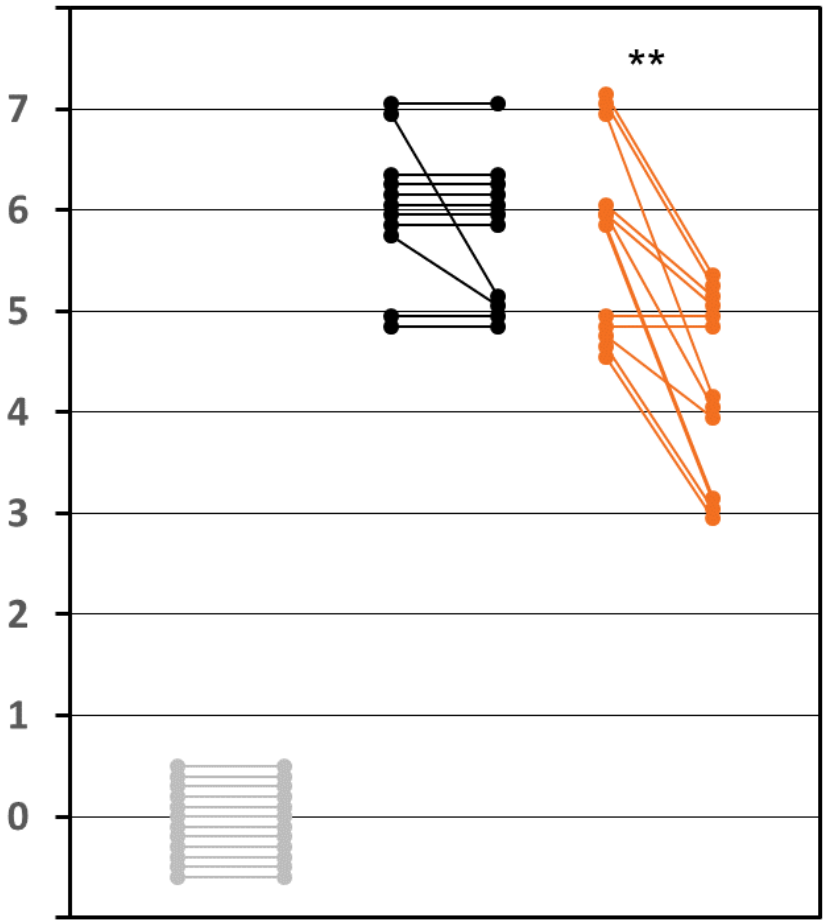

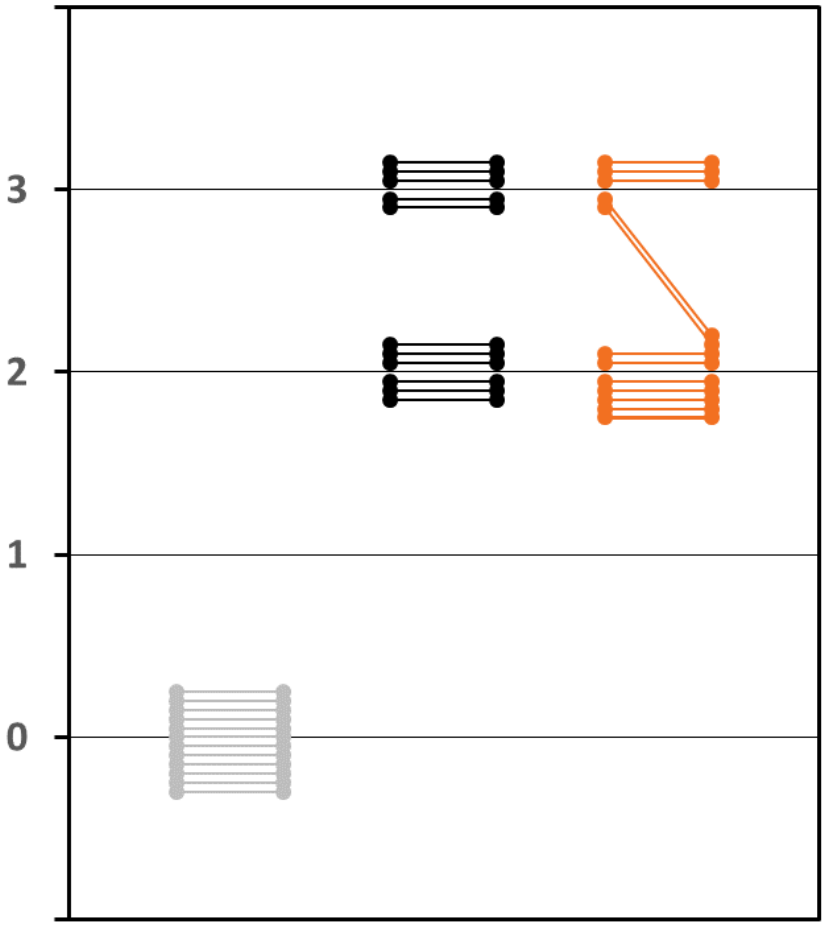

Figure 4

(a) (b)

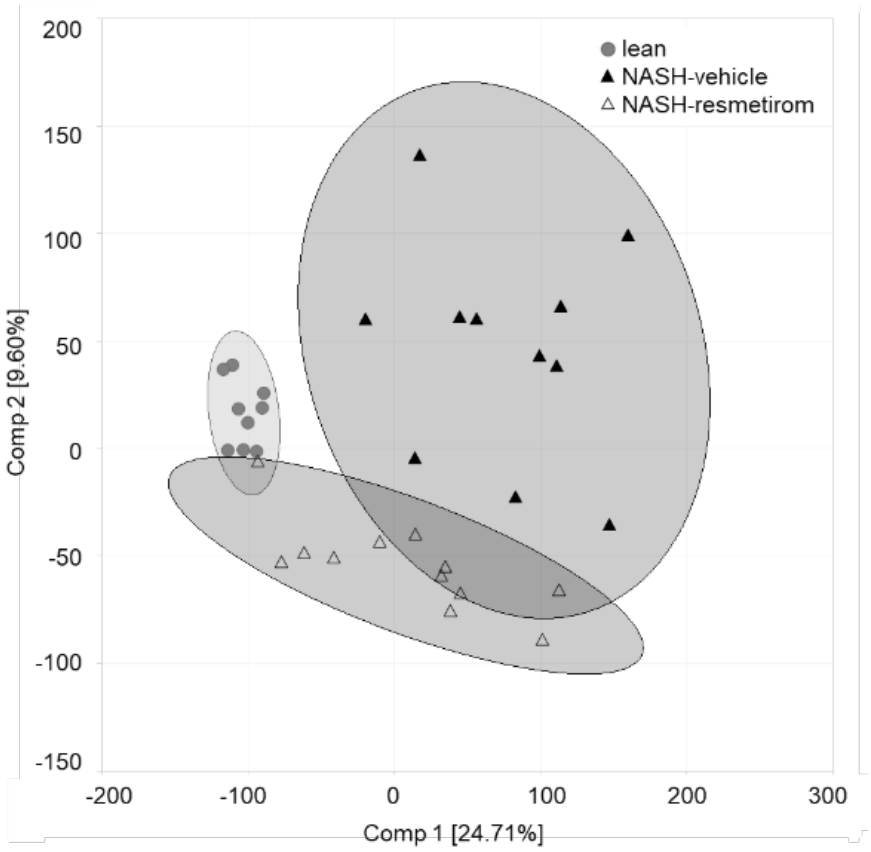

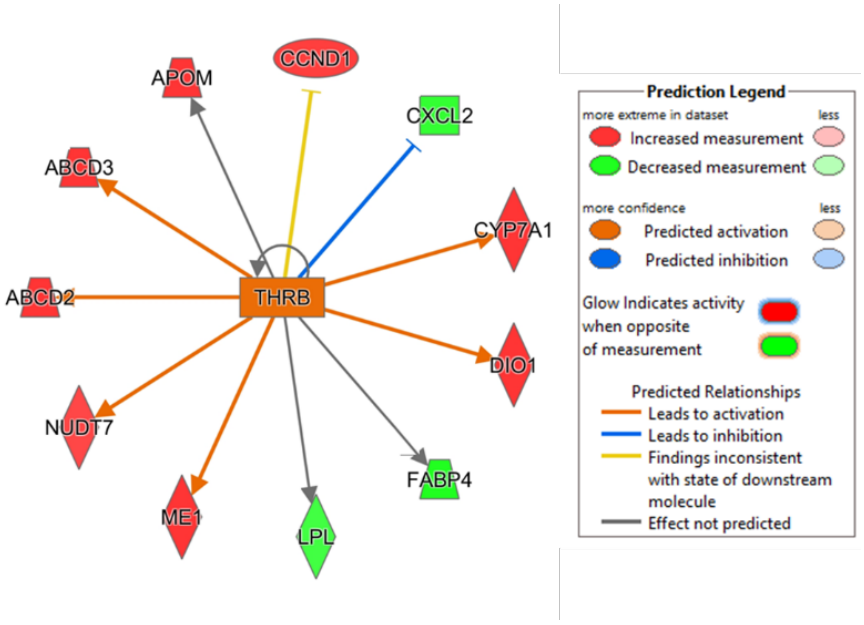

(c)

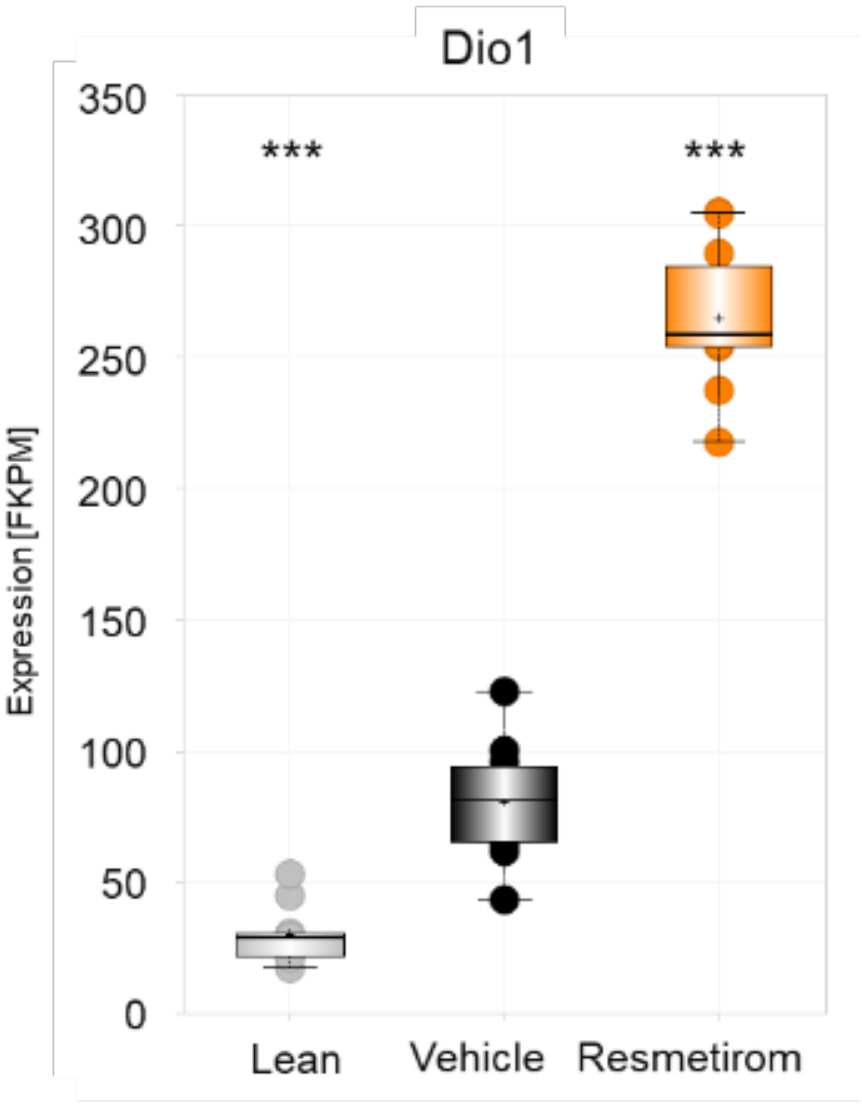

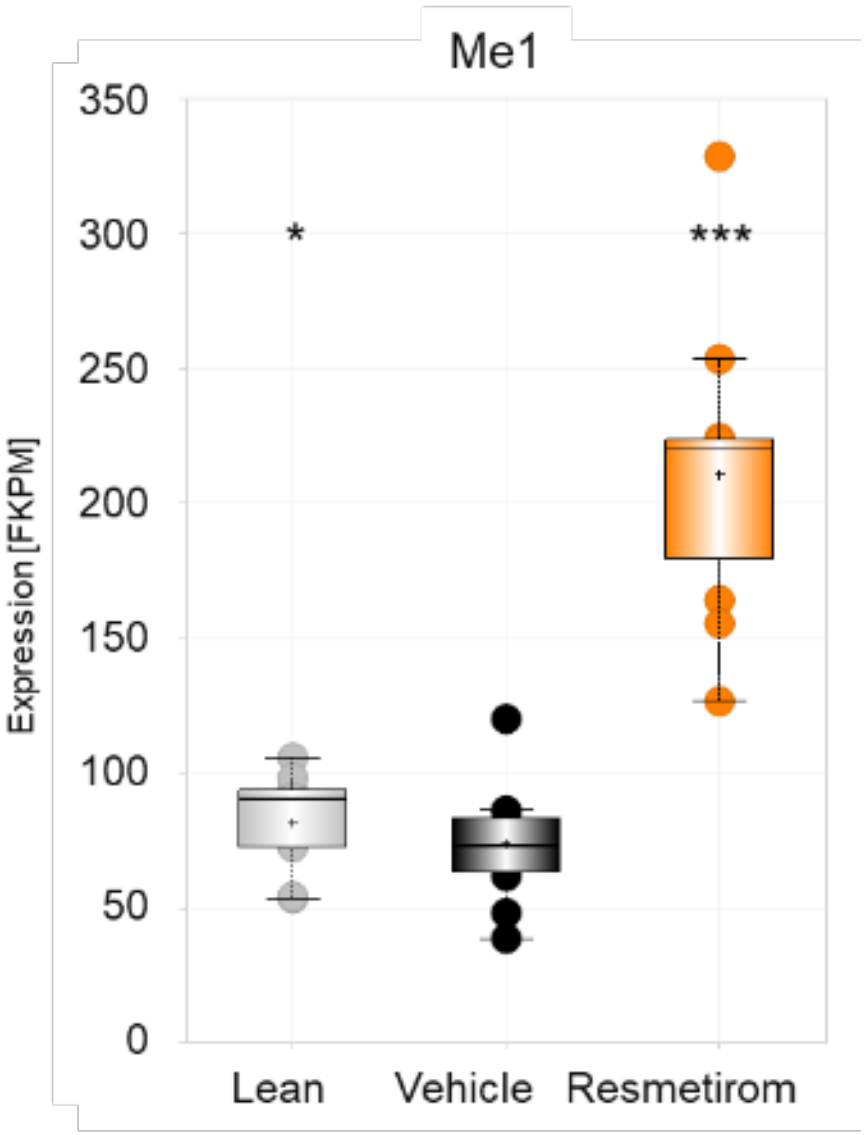

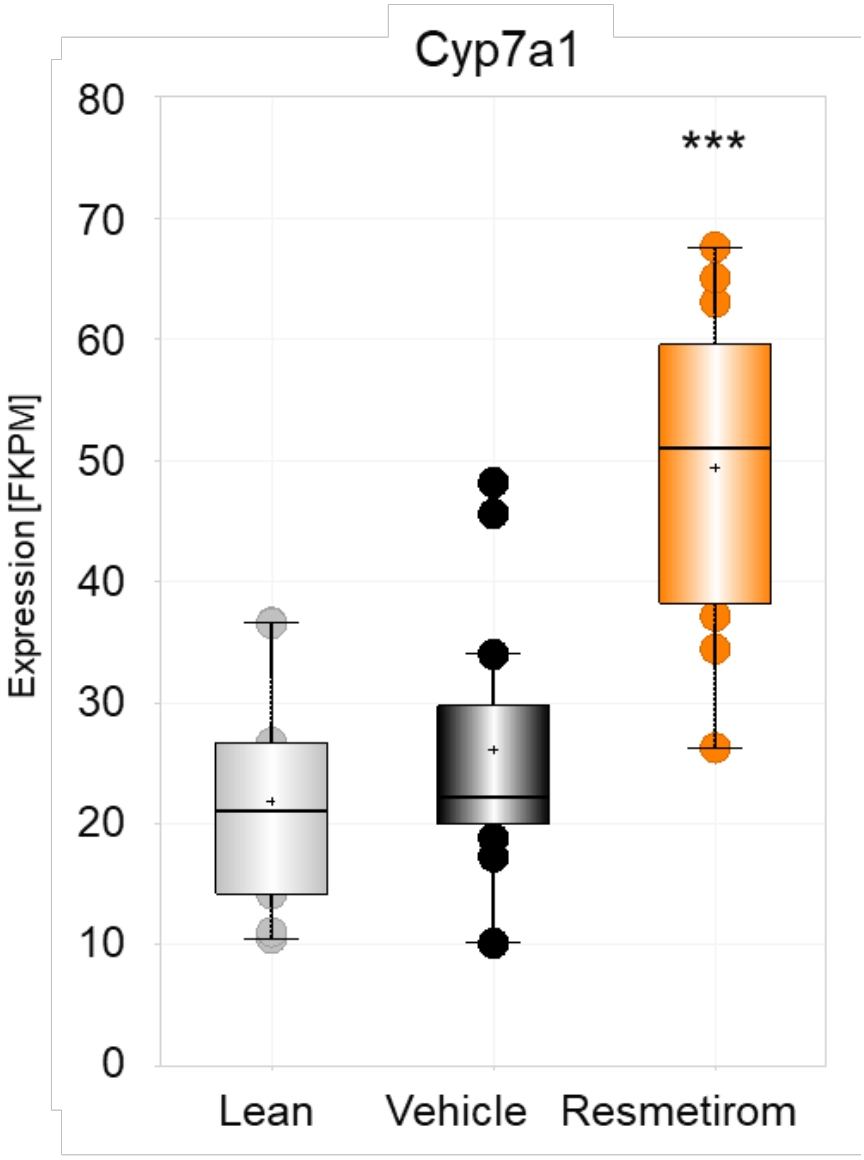

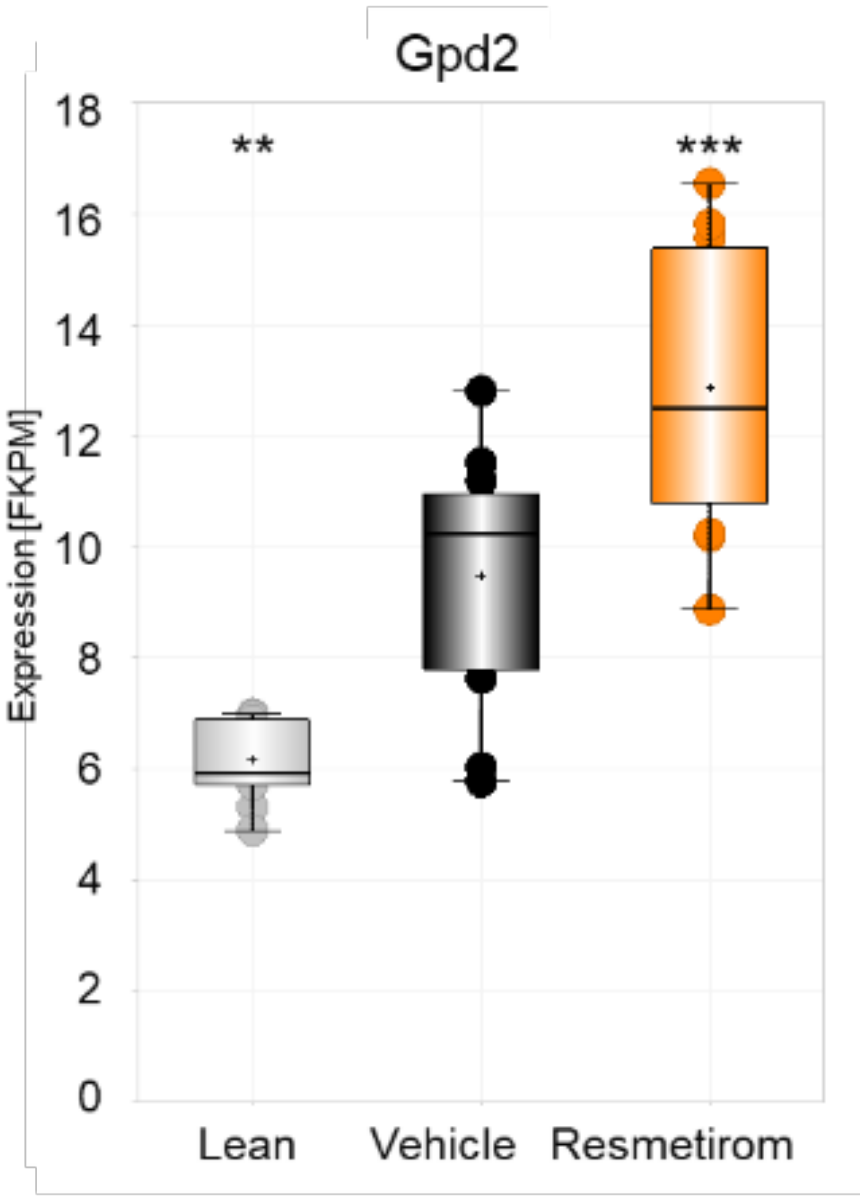

(d)

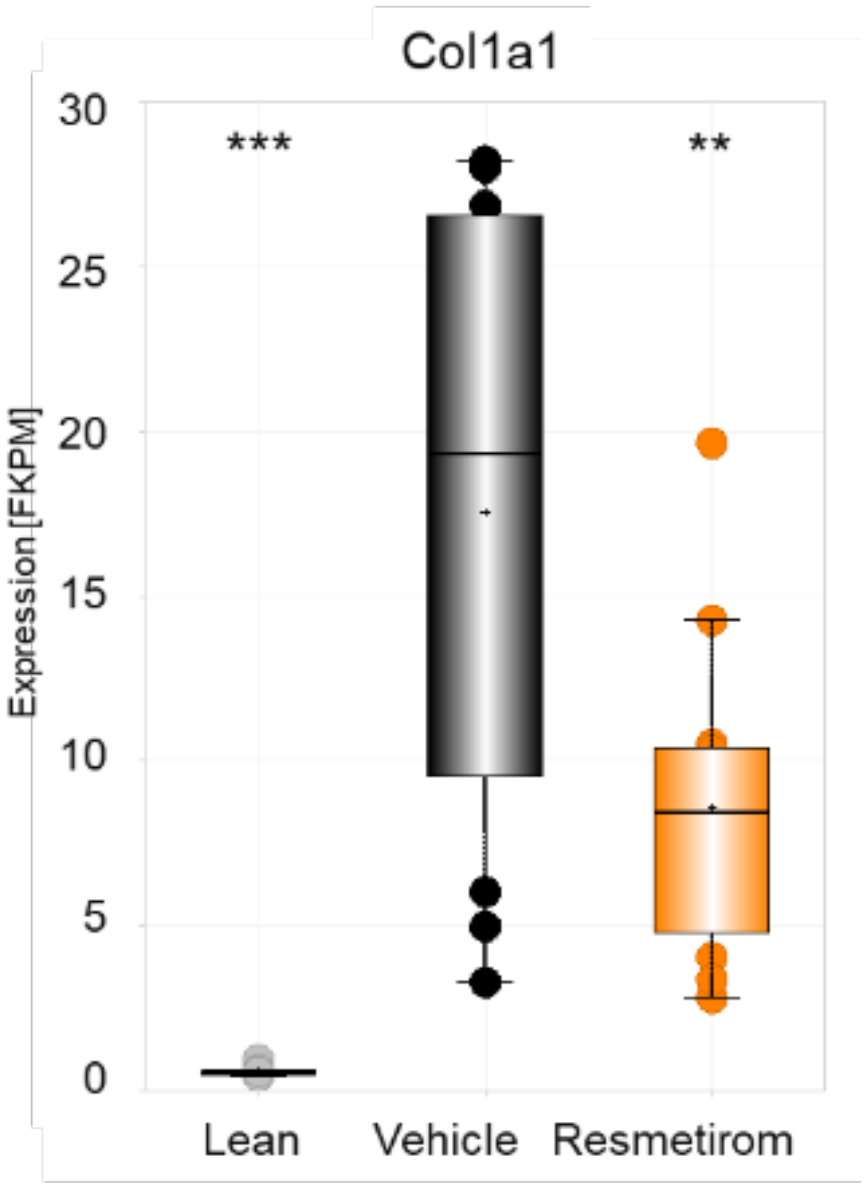

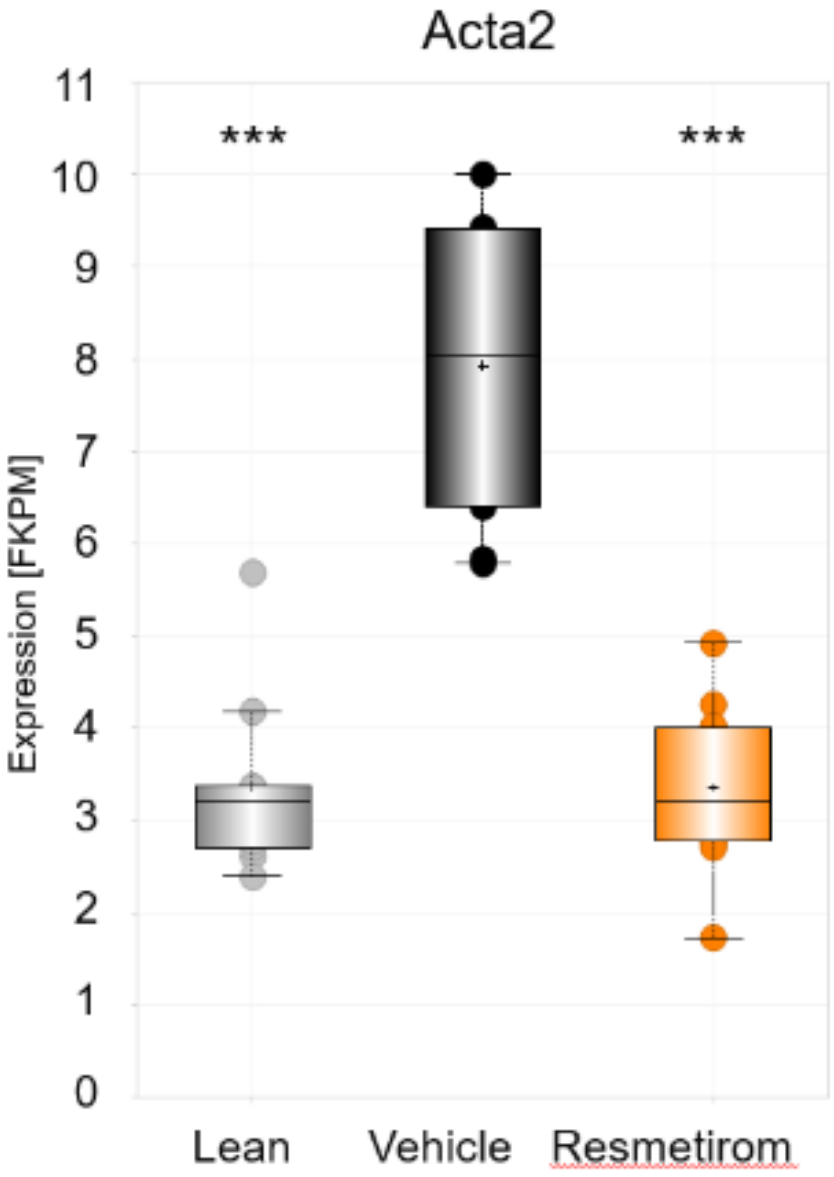

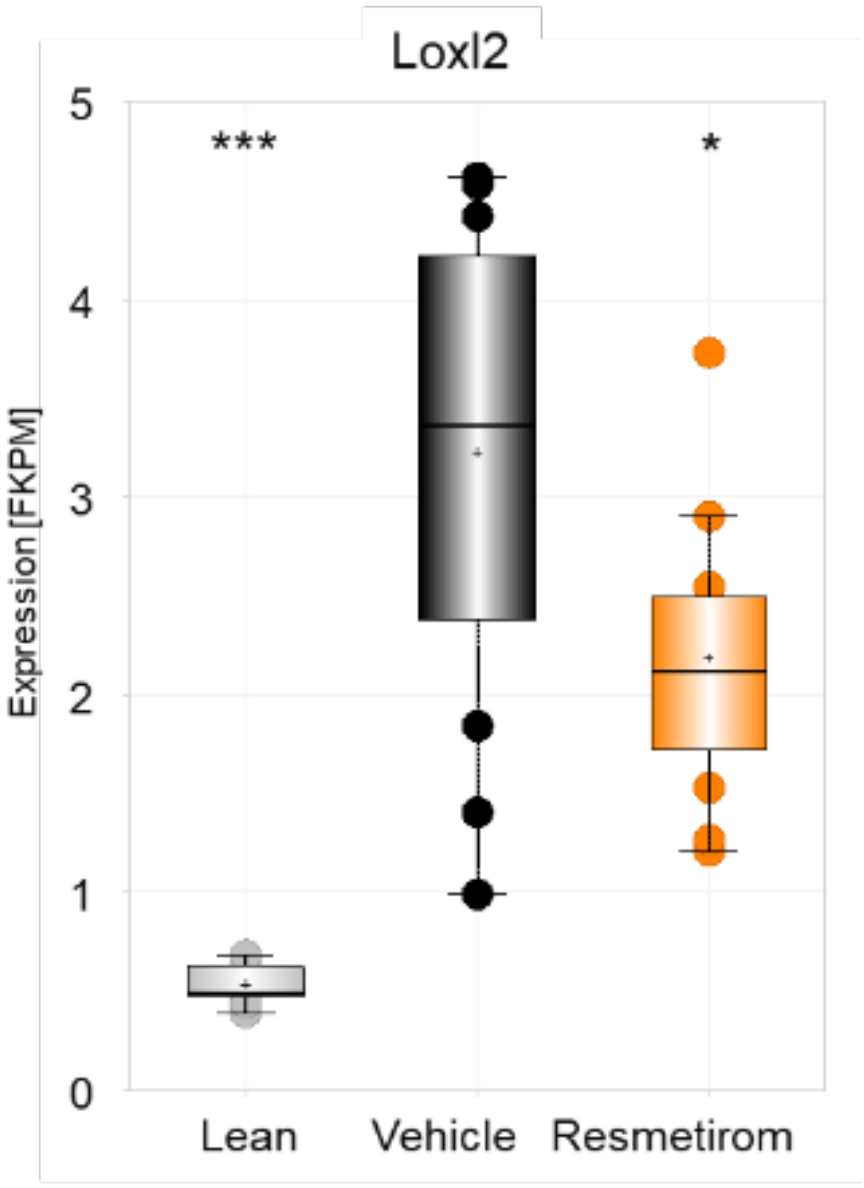

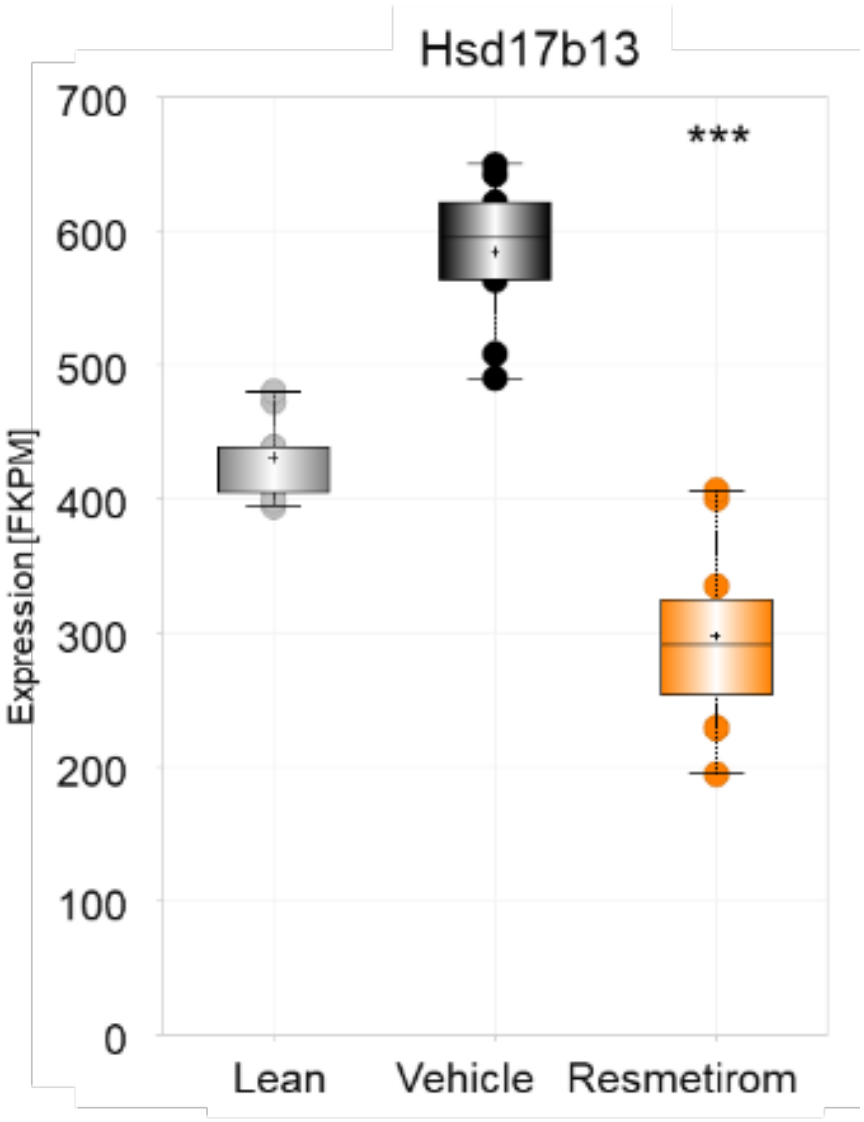

(e)

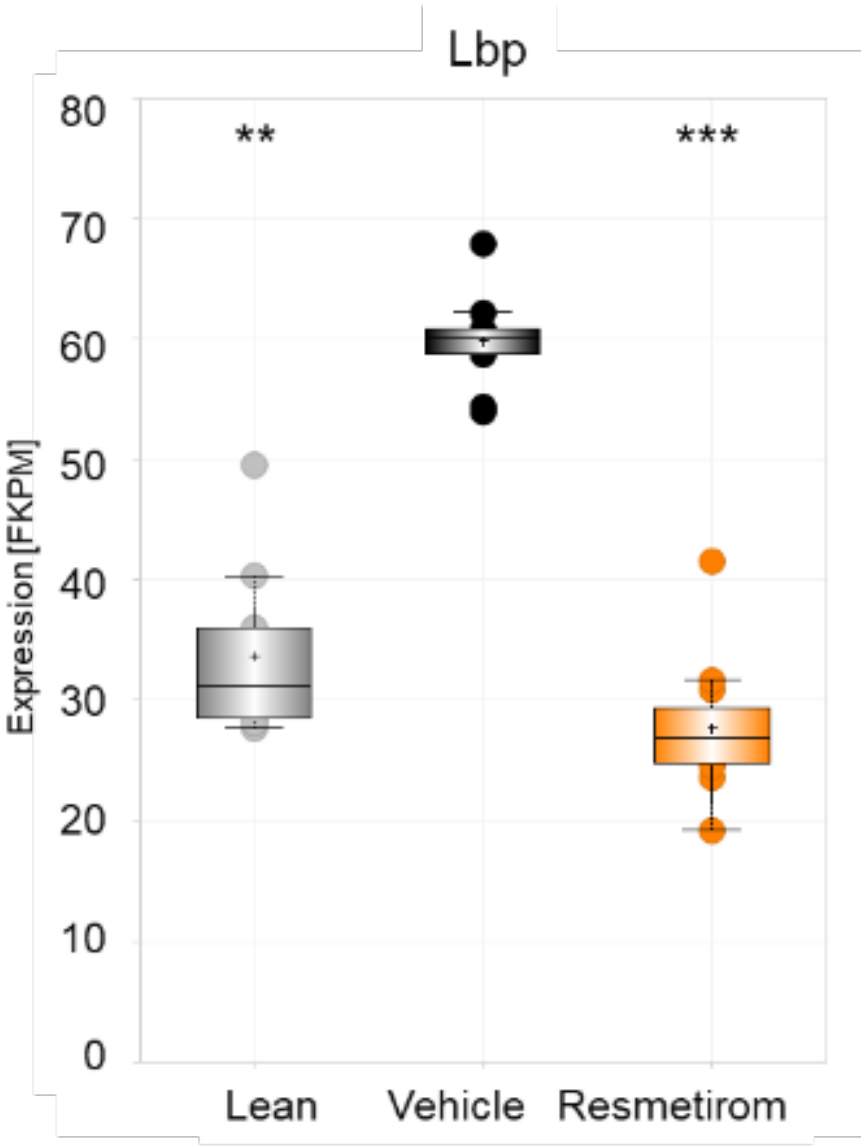

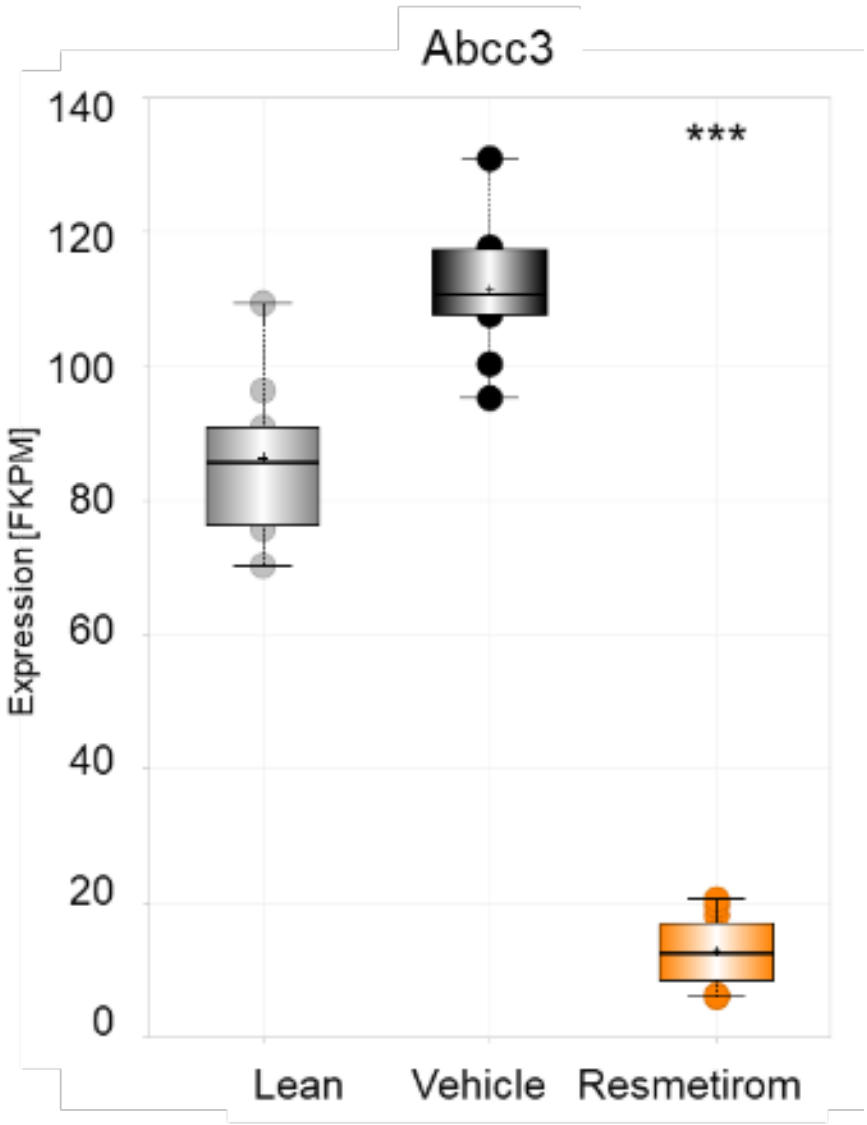

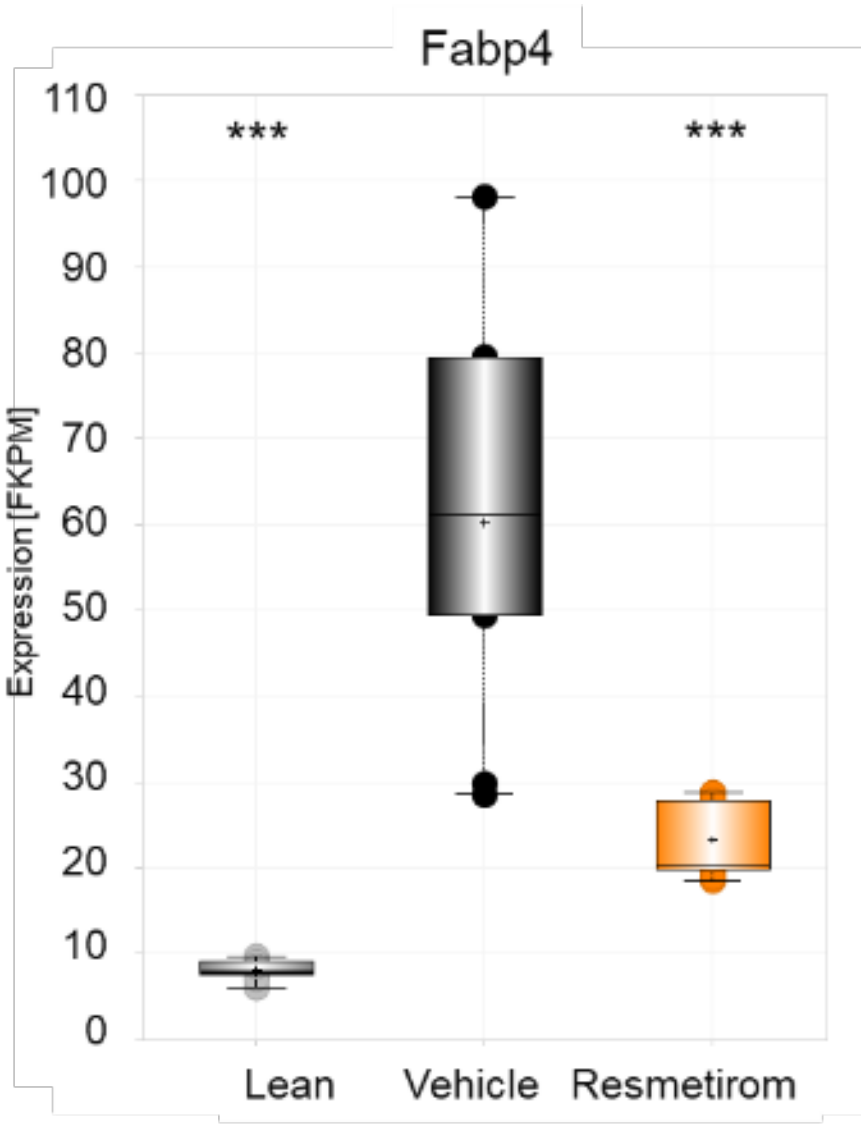

Figure 5